

# Temporal decorrelation of short laser pulses

J. Peatross

*Department of Physics and Astronomy, Brigham Young University, Provo, Utah 84602*

A. Rundquist

*Center for Ultrafast Optical Science, University of Michigan, 2200 Bonisteel Boulevard,  
Ann Arbor, Michigan 48109-2099*

Received May 20, 1997; revised manuscript received August 25, 1997

We describe a unique approach for extracting the temporal profile of ultrashort laser pulses from typical autocorrelation measurements. The use of the constraint that intensity is a nonnegative quantity enables an iterative numerical algorithm to reconstruct pulse shapes in a one-dimensional procedure. With the reconstruction of the intensity profile, the Gerchberg-Saxton algorithm can be used to retrieve the phase of the electric field from a spectral measurement. Because these procedures are carried out in one dimension, they are numerically much faster than two-dimensional techniques such as frequency-resolved optical gating. Their high computational efficiency can save substantial time by constructing good trial solutions for the more accurate but slower procedure of frequency-resolved optical gating. © 1998 Optical Society of America [S0740-3224(98)00301-4]

*OCIS codes:* 320.7100, 070.2590, 070.5010.

## 1. INTRODUCTION

The need to determine the temporal profile of ultrashort laser pulses, both amplitude and phase, has driven a number of innovations in measurement and pulse reconstruction techniques.<sup>1-13</sup> (For a review, see Ref. 13.) For some short pulse applications, a knowledge of the pulse shape is imperative. In high-field applications such as harmonic generation and electron acceleration, pulses tailored to have specific temporal shapes can optimize the results.<sup>14-17</sup> For quantum control of wave packets, the exact nature of the electric fields involved is crucial.<sup>18-20</sup> Various approaches have been used to measure the temporal profile of short laser pulses. One of the simplest and most common approaches is the technique of autocorrelation, in which a replica of the laser pulse combines with the original pulse in some nonlinear process such as second-order harmonic generation.<sup>1-3,13</sup> Although autocorrelation provides useful information such as an approximate duration for the pulse, the measurement is generally regarded as losing the details of the temporal profile. To gain further insight into the characteristics of the laser-pulse profile, one often relies on assumptions and/or additional information obtained from other measurements. For example, to extrapolate the duration of a laser pulse from an auto-correlation trace, one might first assume a pulse shape and then match its width to the measured autocorrelation width.<sup>4</sup> Other methods introduce information from spectral measurements of the laser pulse and/or the correlated signal<sup>4-10,12,13</sup> and may rely on polynomial or other functional interpolations to approximate phase variations.<sup>3</sup> The recently developed technique<sup>8,9,21</sup> of frequency-resolved optical gating (FROG) applies the information obtained from a spectral analysis of the correlated signal to extract in an iterative procedure the temporal charac-

teristics of a pulse. This approach is relatively successful and has recently gained wide use. FROG provides not only a knowledge of the laser-field envelope but also its phase.

In this paper we describe an approach for obtaining the pulse temporal information from a traditional autocorrelation measurement. The extraction of the pulse shape does not depend on additional spectral measurements or assumptions, which classify a form for the pulse. Rather, it takes advantage of a physical principle inherent in an autocorrelation measurement, which, to our knowledge, has not been applied previously to this problem in the form of an iterative algorithm. Specifically, the physical insight is that the laser intensity is a nonnegative quantity, meaning that the accumulated energy deposited on the detector can never decrease in time. The method, which we label temporal information via intensity (TIVI), is different from most pulse characterization schemes in the sense that it can extract amplitude information for the pulse without regard to the phase.

The TIVI method relies on an iterative process denoted the error-reduction algorithm and examined by Fienup *et al.* in the 1970s.<sup>22,23</sup> The algorithm converges for wide ranges of functions (including significantly complicated functions) with good agreement on a linear scale. However, discrepancies can be observed on a logarithmic scale for the forward and trailing edges of a pulse. Moreover, serious ambiguities can arise in some cases where subtle differences in the autocorrelated trace can lead to substantial differences in the reconstructed intensity envelope. In these complicated situations, we have found that a significant improvement to the uniqueness issue can be made by reconstructing simultaneously two distinct pulses while using information from a cross-correlation measurement of the two. In this case, both

pulse forms are unknown. This approach has the added advantage of determining the direction of time flow for both pulses.

As was mentioned, the TIVI method alone does not provide phase information. However, it is possible to extract the phase of a pulse by use of the results of the TIVI method with a measurement of the pulse spectrum. In this case, the phase information of the pulse can be extracted through a one-dimensional application of the Gerchberg–Saxton algorithm.<sup>23–25</sup> (The Gerchberg–Saxton algorithm has previously been used for extracting spatial phase information from two-dimensional images.) We have found that this procedure can be useful in connection with the FROG algorithm. Because they are used in one dimension, the error-reduction and the Gerchberg–Saxton algorithms are many times faster numerically than the FROG algorithm. However, it is our experience that the FROG algorithm is usually able to improve the recovered pulse form. Therefore the approach does not fully substitute for the FROG algorithm, but substantial computing time can be saved by use of the TIVI method with the Gerchberg–Saxton algorithm first followed by the FROG algorithm. In this application, the ambiguities that occasionally occur can be fixed by the FROG algorithm. It turns out that the information necessary to use the TIVI method and the Gerchberg–Saxton algorithm is already present in a second-harmonic-generation FROG measurement. The TIVI method might especially be useful for on-line characterization of low-energy pulses (microjoule or less) where a scan to obtain data for FROG takes significant time.

## 2. TEMPORAL INFORMATION VIA INTENSITY

As illustrated in Fig. 1, a typical autocorrelation measurement employs a beamsplitter to create two identical pulses, which are then brought back together in a nonlinear medium such as a crystal for second-harmonic conversion. If the background light is eliminated, the second-harmonic field produced from mixing the two beams is proportional to the product of the fields as a function of time. One of the pulses can be delayed by an amount  $\tau$  so that the emerging signal takes the form  $E_{\text{sig}}(t, \tau) \sim E(t)E(t - \tau)$ . A detector integrates the intensity of the signal over the entire pulse, and the detected signal is an autocorrelation of the intensity of the original pulses:

$$\text{Sig}(\tau) = \int_{-\infty}^{\infty} I(t)I(t - \tau)dt. \quad (1)$$

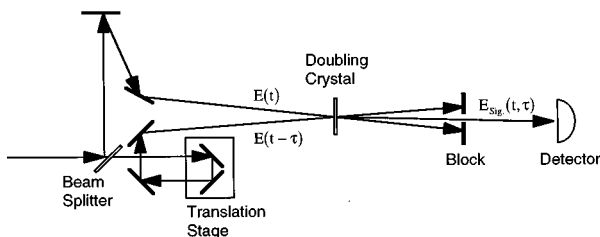


Fig. 1. Schematic of an autocorrelation measurement using second-harmonic generation.

The phase of the electric field is lost since the detector responds to intensity  $I(t) \equiv |E(t)|^2$ . The goal is to recover  $I(t)$  from a knowledge of  $\text{Sig}(\tau)$ . The difficulty of this task becomes apparent after applying the Wiener–Khinchin theorem, from which we find that the Fourier transform of the recorded signal is

$$\text{Sig}(\omega) \equiv F\{\text{Sig}(\tau)\} = |I(\omega)|^2. \quad (2)$$

By writing  $I(\omega)$ , we do not mean the power spectrum of the laser pulse [which we will denote in this paper by  $\tilde{I}(\omega) \equiv |E(\omega)|^2$ ], but rather the Fourier transform of the intensity envelope [i.e.,  $I(\omega) \equiv F\{I(t)\}$ ]. (Throughout this paper, we will denote the Fourier transform of a function by replacing its time argument with a frequency argument.) In general, the Fourier transform of intensity  $I(\omega) = |I(\omega)|\exp[i\phi(\omega)]$  is a complex quantity, whereas only its magnitude is obtained from an autocorrelation measurement. Thus, for a given autocorrelation trace, there exists an infinite number of possible pulses from which it might have derived depending on the form of the phase  $\phi(\omega)$ .<sup>26,27</sup> If the phase is known, then the pulse intensity can be calculated using an inverse Fourier transform:

$$I(t) = F^{-1}\{\sqrt{\text{Sig}(\omega)} \exp[i\phi(\omega)]\}. \quad (3)$$

It is this missing knowledge of  $\phi(\omega)$  that supports the viewpoint that the details of the temporal profile of the pulse are lost in the measurement. In this case, assumptions are often employed in an effort to extract meaningful information about the pulse.<sup>4</sup> For example, it may be assumed that the pulse shape is Gaussian or a squared hyperbolic secant, and this can provide a proportionality factor between the duration of the pulse and the duration of the autocorrelation trace. Nevertheless, the results vary with the particular assumption invoked, and there remains an uncertainty as to whether the pulse is simple in shape or misshapen.

The ambiguity in choosing  $\phi(\omega)$  in Eq. (3) is to a large extent eliminated if one also invokes the restriction that  $I(t)$  is a real, nonnegative quantity. In other words, as the light strikes the detector, never does it remove energy that was previously deposited. The requirement that  $I(t)$  be real is satisfied if  $\phi(-\omega) = -\phi(\omega)$ . [Note that since  $\text{Sig}(\tau)$  is even, we automatically have  $|I(-\omega)| = |I(\omega)|$ ]. While it is difficult to know *a priori* what  $\phi(\omega)$  should be to satisfy the criterion  $I(t) = |I(t)| \geq 0$ , an iterative scheme can be used to converge to it. This iterative technique has been studied by Fienup *et al.* and is called by them the error-reduction algorithm.<sup>22,23</sup> To our knowledge, our work is the first to recognize the algorithm's application to the recovery of laser-pulse shapes from autocorrelation measurements. Figure 2 shows the algorithm schematically. A Fourier transform is applied to a trial solution for  $I(t)$ . The magnitude of  $I(\omega)$  is then replaced by its known value [i.e.,  $[\text{Sig}(\omega)]^{1/2}$ ] without disturbing the phase. An inverse Fourier transform is then applied to obtain a new function  $I(t)$ , and any portion that is negative is set to zero to create the new trial solution. Note that if the trial solution  $I(t)$  is chosen to be real, then the new trial solution will also be real automatically. The procedure continues until the algorithm converges to a pulse that is nonnegative upon emerging

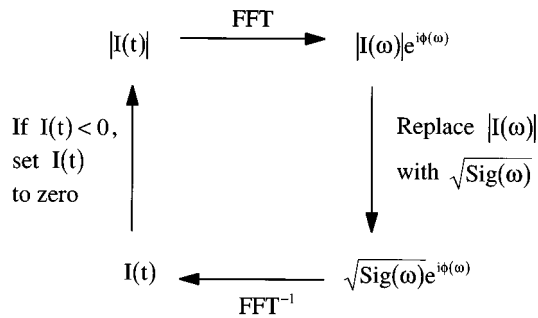


Fig. 2. Schematic of the TIVI method, which is able to recover the intensity temporal profile.

from the frequency domain. It has been shown that the error reduction algorithm never increases the error but, in the worst case, can only stagnate at a value. Otherwise it continually decreases the error value at every iteration. It should also be noted that while the original FROG algorithm was improved by performing gradient searches on the FROG error, the error reduction algorithm has been shown to be a single-step gradient search in one dimension.<sup>23</sup>

A more robust and rapid means of convergence, at least in the first several iterations, is often achieved by replacing negative portions of  $I(t)$  with their differences from their values on the previous iteration; this approach has been named the input-output algorithm by Fienup *et al.*<sup>23</sup> because it treats the first three steps of the error-reduction algorithm as a nonlinear black box, and it adjusts the input on every iteration until the output fits the constraints in both Fourier domains. A different approach, which often helps with convergence, is to overcorrect by  $\sim 20\%$  when adjusting the magnitude of  $I(\omega)$  to its known value. We generally use one of these methods for initial convergence and follow it with the procedure indicated in Fig. 2, which often improves the solution. Another method that works well is to intermingle the approaches on alternate iterations, following what Fienup *et al.* call the hybrid input-output algorithm.<sup>23</sup>

As a measure of how well the algorithm converges to a solution, two methods for calculating error can be used to monitor how well the function is converging: Upon emergence from the frequency domain, the fraction of  $I(t)$  that is negative can be computed, and upon emergence from the time domain, the deviation of  $|I(\omega)|$  from  $[\text{Sig}(\omega)]^{1/2}$  can be computed. We generally use the latter method and monitor the root-mean-square deviation of  $|I(\omega)|$  from  $[\text{Sig}(\omega)]^{1/2}$  on each iteration.

### 3. APPLICATION OF TEMPORAL INFORMATION VIA INTENSITY

In Fig. 3(a), we show three autocorrelation traces (synthetic data) having identical full widths at half-maximum but arising from three different functions, namely, a Gaussian, a squared hyperbolic secant, and a squared sinc function. Figure 3(b) shows the functions that were used to form the autocorrelation traces together with the reconstructed traces obtained with the TIVI method. The curves are indistinguishable from the original curves. As is evident in Fig. 3(b), the original curves have differ-

ent widths even though their autocorrelation widths are the same. This points out the possible error introduced by assuming a functional form; the often-used squared hyperbolic secant gives the shortest pulse duration. The TIVI method is an impartial means of finding the pulse duration, and it is less computationally intensive than performing a numerical fit of a particular functional form to the autocorrelation data.

Figures 4(a)–4(c) give examples of autocorrelation traces arising from more exotic pulse forms. The curves in Figs. 4(d)–4(f) show the reconstructed pulses obtained from the TIVI method along with the original curves used to synthesize the autocorrelation traces. There remains a time-reversal ambiguity (as well as an unimportant translation ambiguity), which we artificially adjust to

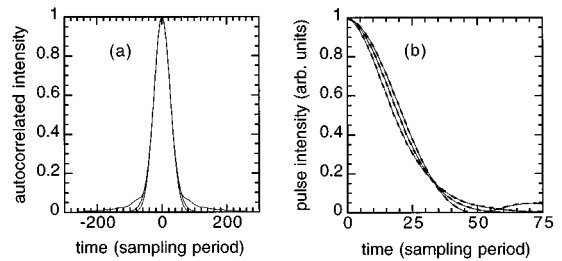


Fig. 3. (a) Autocorrelation traces arising from Gaussian, squared hyperbolic secant, and squared sinc pulses. (b) Original pulses (thin solid curves) and reconstructed pulses obtained by the TIVI method (dashed curves).

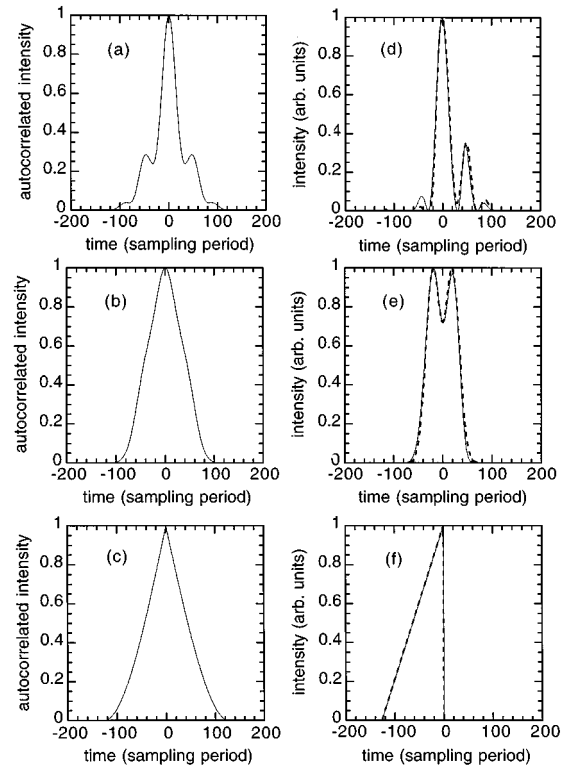


Fig. 4. (a)–(c) Autocorrelation traces arising from three arbitrarily chosen pulse shapes. (d)–(f) Original pulses (thin solid curves) and reconstructed pulses obtained by the TIVI method (dashed curves). Note that in (d) the reconstruction method failed to recover the small bump on the left.

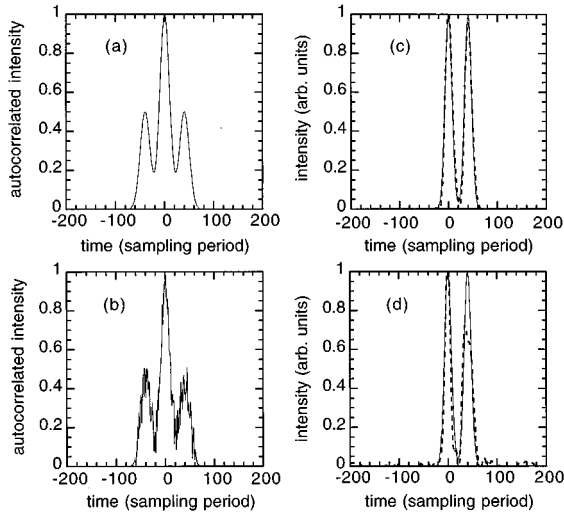


Fig. 5. (a) Autocorrelation trace of an arbitrarily chosen pulse shape. (b) The same autocorrelation trace with a random additive noise of 25% (fluctuation range). (c) Original pulse (thin solid curve) and reconstructed pulse obtained by the TIVI method (dashed curve) without noise. (d) Original pulse (thin solid curve) and reconstructed pulse obtained by the TIVI method (dashed curve) in the presence of noise.

have the correct sense so that the reconstructed pulses can be more easily compared with the original curves. Figure 5(a) shows an autocorrelation trace of another pulse and Fig. 5(b) shows the same autocorrelation trace to which 25% (peak to valley) random noise has been added. Figure 5(c) shows the reconstructed pulse obtained from the TIVI method along with the original curve used to make the autocorrelation trace in Fig. 5(a). Figure 5(d) shows the reconstruction obtained from the autocorrelation trace with the added noise. Before reconstruction, the autocorrelation trace was smoothed and symmetrized. Although the reconstruction is degraded somewhat in the presence of noise, the TIVI method is still able to reconstruct most of the main features.

Figures 6(a) and 6(b) show examples of autocorrelation signals for which the TIVI method generates ambiguous results. Figures 6(c) and 6(d) show reconstructed pulses for the autocorrelation traces that have converged to wrong results. Whether the iterative process converges to the correct shape or to an ambiguous one (when existent) can depend on the initial trial solution. We often use for a guess the sum of several Gaussian curves with randomly chosen widths and positions. A simple triangle can also be a suitable initial guess, and a single triangle was used as a trial solution for most of the figures in this paper. The choice of an even trial solution is often disadvantageous since there is nothing in the algorithm that breaks the symmetry (other than numerical noise) when an asymmetric solution is needed. Thus the algorithm can stagnate unless the solution is in fact even.

The examples of ambiguities<sup>28-30</sup> in Fig. 6 illustrate a significant difficulty with the method since this problem occurs for  $\sim 10\%$  of the arbitrary pulses that we have examined. In fact, the TIVI method converges to ambiguous results for the important pulse shape of strong third-order dispersion. Nevertheless, when ambiguities (or

low-error stagnations) occur for reconstructed solutions, they often significantly resemble each other as seen in the figures.<sup>22</sup> The following section describes a technique for minimizing the problem of ambiguities.

Figure 7 shows the calculated error as a function of the number of iterations for the curves seen in Figs. 4 and 6. The error is shown for up to 1000 iterations, but the reconstructed figures correspond in all cases to 25 iterations. Even though the error improves with further iterations, the recovered curves do not significantly change on a linear scale. Figure 7(b) indicates that the recovered curves in Fig. 6 are true ambiguities rather than stagnations since the error decreases down to the noise level of the machine.

#### 4. TEMPORAL INFORMATION VIA INTENSITY WITH CROSS-CORRELATION INFORMATION

When two pulses combine in a cross-correlation measurement, the information leads to a knowledge of the intensity profile of both pulses if one of them is already known. The signal measured from the cross-correlated pulses is

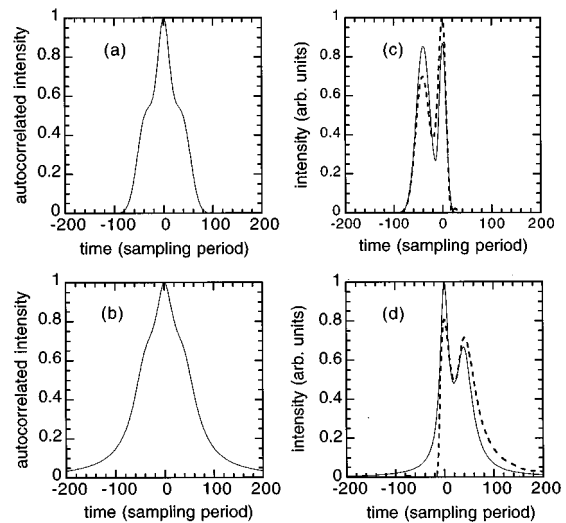


Fig. 6. (a), (b) Autocorrelation traces arising from pulses for which reconstruction fails. (c), (d) Original pulses (thin solid curves) and reconstructed pulses obtained by the TIVI method (dashed curves).

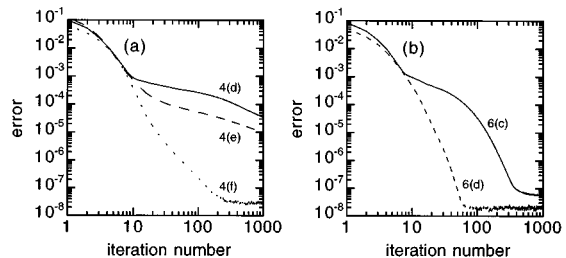


Fig. 7. (a) Errors calculated for the curves seen in Fig. 4(d) (solid curve), Fig. 4(e) (long-dashed curve), and Fig. 4(f) (short-dashed curve). (b) Errors calculated for the curves seen in Fig. 6(c) (solid curve) and Fig. 6(d) (dashed curve).

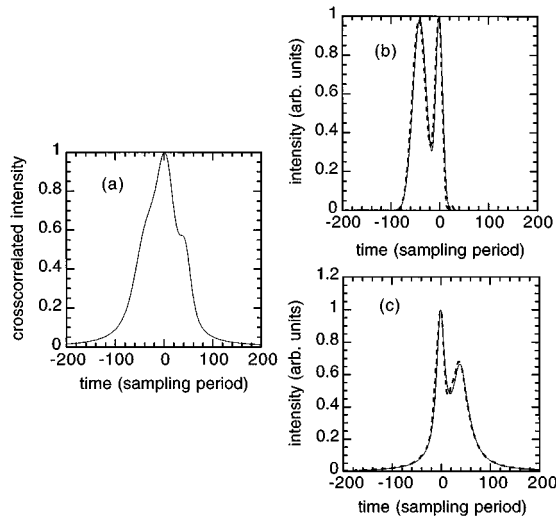


Fig. 8. (a) Cross-correlation trace arising from the two pulses seen in Fig. 6. (b), (c) Original pulses (thin solid curves) and reconstructed pulses (dashed curves) obtained by the TIVI method while utilizing the information in the cross-correlation trace.

$$\text{Sig}_{12}(\tau) = \int_{-\infty}^{\infty} I_1(t)I_2(t - \tau)dt, \quad (4)$$

and the Fourier transform of the measurement gives

$$\text{Sig}_{12}(\omega) \equiv F\{\text{Sig}_{12}(\tau)\} = I_1(\omega)I_2^*(\omega). \quad (5)$$

Thus, if  $I_1(\omega)$  is known,  $I_2(\omega)$  can be obtained and vice versa. If it is desired to produce either intensity profile from a knowledge of the other, the application of Eq. (5) is limited to pulses with features of comparable temporal duration so that  $I_1(\omega)$  and  $I_2(\omega)$  tend to zero with similar rates.

Now consider the case in which two distinct pulses are both unknown. Suppose that the autocorrelation signal  $\text{Sig}_{11}(\tau)$  of one of the pulses is known along with a cross-correlation measurement involving the second pulse  $\text{Sig}_{12}(\tau)$ . The autocorrelation signal of the second pulse might also be measured, or it can be obtained instead through the relation

$$\text{Sig}_{11}(\omega)\text{Sig}_{22}(\omega) = |\text{Sig}_{12}(\omega)|^2. \quad (6)$$

In the laboratory, the second pulse might be created by splitting off a portion of the first pulse and sending it through a dispersive element so long as the duration does not increase dramatically (say, far beyond a factor of 2). To obtain the intensity profile of both pulses from the above measurements, a few iterations of the TIVI method can be applied to the first pulse, whereupon the result in conjunction with Eq. (5) provides a trial solution for an application of the TIVI method on the second pulse (a few iterations). Equation (5) can then be used again to provide a new trial solution for the first pulse, and the process repeats until both solutions converge. Figure 8(a) shows the cross-correlation signal corresponding to the pulses used in Fig. 6. Figures 8(b) and 8(c) show the recovered pulses for which the cross-correlation information was used. As is apparent, the ambiguities that occur when recovering each pulse individually are removed. In addition, the sense of time flow is recovered. The possi-

bility of ambiguities may persist in the cross-correlation case although with a far reduced likelihood.

## 5. PHASE RETRIEVAL WITH THE GERCHBERG-SAXTON ALGORITHM

The TIVI method can recover the temporal amplitude of a pulse, but it does not retrieve the phase. A knowledge of the amplitude offers an interesting possibility for finding the phase if the spectral content of a pulse is known [i.e.,  $\tilde{I}(\omega) \equiv |E(\omega)|^2 \neq I(\omega)$ ]. The Gerchberg-Saxton algorithm has been used for recovering two-dimensional spatial phase information of images when the amplitude of the field is known at near- and far-field planes.<sup>24,25</sup> We have applied the Gerchberg-Saxton algorithm in one dimension to recover the phase of pulses for which the temporal and spectral amplitudes are known. Figure 9 displays a schematic of the procedure. A trial electric field having the known amplitude is transformed to the frequency domain. The amplitude of the field is adjusted to agree with the known frequency amplitude while leaving the phase unaltered. The field is then transformed back to the time domain where the amplitude is again adjusted while leaving the phase unaltered. The procedure is repeated until convergence is achieved. Figures 10(a) and 10(b) show, respectively, the amplitude and phase of a pulse recovered with the TIVI method followed by the Gerchberg-Saxton algorithm. It is assumed that the spectral amplitude is known. The algorithms together took a total of 100 iterations [200 fast Fourier transforms (FFTs)]. The original pulse is shown with each curve as a reference. The pulse has arbitrarily chosen multiple peaks with an added amount of self-phase modulation ( $B$  integral of 1). Figures 10(c) and 10(d) show the same pulse recovered by the second-harmonic FROG algorithm. This procedure took 35 iterations ( $35 \cdot 128 \cdot 2 = 8960$  FFTs). The curves are indistinguishable in amplitude, and only the phase differs at the wings of the pulse where the amplitude goes to zero.

It should be noted that the Gerchberg-Saxton algorithm is able to recover pulses only to the extent that the temporal profile recovered by the TIVI method is close to the actual pulse (with amplitude accuracy within  $\sim 10\%$  of the peak value). The fact that the square root is taken of the reconstructed intensity profile before the

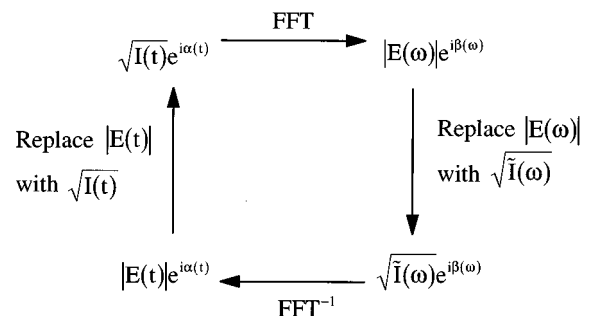


Fig. 9. Schematic of the Gerchberg-Saxton algorithm applied to the problem of recovering the phase of the electric field.

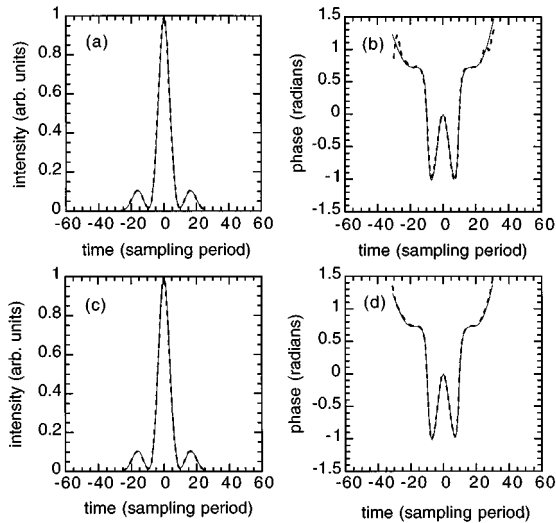


Fig. 10. (a) Original amplitude (thin solid curve) and reconstructed amplitude (dashed curve) obtained by the TIVI method. (b) Original phase (thin solid curve) and reconstructed phase (dashed curve) obtained by the Gerchberg–Saxton algorithm. (c) Original amplitude (thin solid curve) and reconstructed amplitude (dashed curve) obtained by the FROG algorithm. (d) Original phase (thin solid curve) and reconstructed phase (dashed curve) obtained by the FROG algorithm.

Gerchberg–Saxton algorithm is used means that small errors are enhanced, and this can occasionally frustrate the procedure.

## 6. DISCUSSION

An interesting application of the TIVI method and the Gerchberg–Saxton algorithm is to use them for creating a preliminary solution for injection into the FROG algorithm. The advantage is that very substantial numbers of iterations of the FROG algorithm can be saved at a time cost of less than one FROG iteration. In the event that the TIVI method and the Gerchberg–Saxton algorithm stagnate or converge to an incorrect solution, their injection into the FROG algorithm often still benefits since such solutions often resemble the true solution. Typically, in the case with no added noise, the TIVI/Gerchberg–Saxton (TIVI–GS) method takes a few seconds to converge, whereupon the second-harmonic FROG algorithm is able to reach complete convergence after 5 iterations. If the FROG algorithm is given a random guess, it typically takes between 20 and 50 iterations to converge similarly. The time savings is significant since iteration time for FROG is between 3 and 5 s (on a 180-MHz Power-Macintosh) with a grid size of 128. The time savings would be particularly significant for larger grid sizes. We have also found that in the presence of as much as 10% noise on the autocorrelation and power spectrum separately, the TIVI method still provides a good initial guess for the FROG algorithm. In many cases, the TIVI method does a reasonable job by itself in characterizing the amplitude and phase of a pulse. Only in applications for which the accuracy needed in the phase of a measurement is critical is the FROG algorithm essential to clean up the results of the TIVI method.

In Fig. 11 we show the application of the TIVI–GS algorithm to create a trial solution for the FROG algorithm. We added 10% noise separately to the autocorrelation, the power spectrum, and the FROG trace. Figure 11(a) shows the FROG trace of the original (noise-free) pulse. Figure 11(b) shows the reconstruction of the TIVI–GS algorithm alone, and Fig. 11(c) shows the reconstruction of the TIVI–GS followed by the FROG algorithm. Using Fig. 11(b) as an initial guess in FROG meant that the FROG algorithm required only 5 iterations (1480 FFTs total with the TIVI–GS algorithm). If we run the FROG algorithm with a random guess, the output is the same but the number of iterations is typically 20–30 (5000–8000 FFTs total). Even on a relatively fast computer, it appears that the addition of the TIVI–GS step saves significant time.

The information necessary to use the TIVI method is present in a second-harmonic FROG trace and is easily extracted by integrating across the frequency dimension. The information necessary to use the Gerchberg–Saxton algorithm [i.e., the power spectrum of the pulse denoted  $\tilde{I}(\omega) \equiv |E(\omega)|^2$ ] can be obtained through an independent measurement, but it can also be extracted from the FROG trace. An integration of the FROG trace over the time domain yields the autoconvolution of the power spectrum. The inverse Fourier transform of this autoconvolution curve is  $\tilde{I}^2(t)$ , where this unusual function is defined by  $\tilde{I}(t) \equiv F^{-1}\{\tilde{I}(\omega)\}$ . Thus, if the correct sign can be chosen when taking the square root of  $\tilde{I}^2(t)$  at each time  $t$ , the power spectrum of the pulse  $\tilde{I}(\omega)$  can be obtained from the FROG trace and eliminate the need for a separate measurement. We have found that choosing the sign so that  $\tilde{I}(t)$  is smooth and continuous is a good means of taking the square root. The additional criterion  $\tilde{I}(\omega) = |\tilde{I}(\omega)| \geq 0$  can also be used to ensure the correct answer.

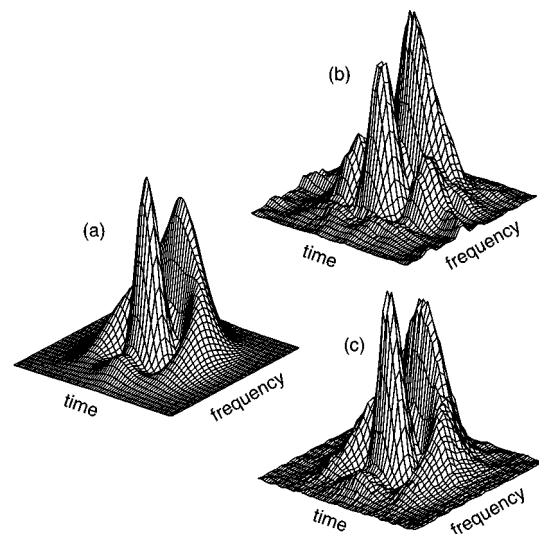


Fig. 11. (a) Synthesized FROG trace. (b) FROG trace generated after applying TIVI–GS to the autocorrelation trace and power spectrum with 10% noise, respectively. (c) Trace generated by the FROG algorithm using the result of TIVI–GS as a trial solution.

## 7. SUMMARY

Our numerical investigations have shown that it is possible to recover temporal amplitude information from traditional autocorrelation traces by means of the constraint that intensity is a nonnegative quantity. Unlike other approaches for recovering pulse forms, the iterative method works on the pulse intensity rather than on the field. We have identified the problem of occasional ambiguities. This difficulty can be removed to a large extent by reconstructing two unknown pulses under the constraint of a cross-correlation measurement made between the pulses. With the recovery of the pulse amplitude, the Gerchberg–Saxton algorithm can be used in connection with a measurement of the power spectrum to recover the phase of the electric field. These methods are found to save significant computing time when used to generate a trial solution for the more robust FROG algorithm. Because of their computational efficiency, the TIVI method and the Gerchberg–Saxton algorithm may be particularly useful for on-line measurements, especially for low-energy pulses, for which the generation of FROG data requires significant time. We have not investigated the possibility that the TIVI method and Gerchberg–Saxton algorithm might be useful in connection with types of FROG other than that based on second-harmonic generation. In future work, we plan to examine the effectiveness of these techniques when applied to experimental data.

## ACKNOWLEDGMENTS

We acknowledge J. Fienup for helpful dialogue. We also acknowledge help from E. Zeek and D. Fittinghoff.

## REFERENCES

1. H. P. Weber, "Method for pulsewidth measurement of ultrashort light pulses generated by phase-locked lasers using nonlinear optics," *J. Appl. Phys.* **38**, 2231–2234 (1967).
2. E. B. Treacy, "Measurement and interpretation of dynamic spectrograms of picosecond light pulses," *J. Appl. Phys.* **42**, 3848–3858 (1971).
3. T. Andersson and S. T. Eng, "Determination of the pulse response from intensity autocorrelation measurements of ultrashort laser pulses," *Opt. Commun.* **47**, 228–290 (1983).
4. J.-C. Diels, J. J. Fournaine, I. C. McMichael, and F. Simoni, "Control and measurement of ultrashort pulse shapes (in amplitude and phase) with femtosecond accuracy," *Appl. Opt.* **24**, 1270–1282 (1985).
5. K. Naganuma, K. Mogi, and H. Yamada, "General method of ultrashort light pulse chirp measurement," *IEEE J. Quantum Electron.* **25**, 1225–1233 (1989).
6. J. L. A. Chilla and O. E. Martinez, "Direct determination of the amplitude and phase of femtosecond light pulses," *Opt. Lett.* **16**, 39–41 (1991).
7. C. Yan and J.-C. Diels, "Amplitude and phase recording of ultrashort pulses," *J. Opt. Soc. Am. B* **8**, 1259–1263 (1991).
8. R. Trebino and D. J. Kane, "Using phase retrieval to measure the intensity and phase of ultrashort pulses: frequency-resolved optical gating," *J. Opt. Soc. Am. A* **10**, 1101–1111 (1993).
9. J. Paye, M. Ramaswamy, J. G. Fujimoto, and E. P. Ippen, "Measurement of the amplitude and phase of ultrashort light pulses from spectrally resolved autocorrelation," *Opt. Lett.* **18**, 1946–1948 (1993).
10. M. T. Kauffman, W. C. Banyai, A. A. Godil, and D. M. Bloom, "Time-to-frequency converter for measuring picosecond optical pulses," *Appl. Phys. Lett.* **64**, 270–272 (1994).
11. B. S. Prade, J. M. Schins, E. T. J. Nibbering, M. A. Franco, and A. Mysyrowicz, "A simple method for the determination of the intensity and phase of ultrashort optical pulses," *Opt. Commun.* **113**, 79–84 (1994).
12. J. K. Rhee, T. S. Sosnowski, A. C. Tien, and T. B. Norris, "Real-time dispersion analyzer of femtosecond laser pulses with use of a spectrally and temporally resolved upconversion technique," *J. Opt. Soc. Am. B* **13**, 1780–1785 (1996).
13. J.-C. Diels, *Ultrashort Laser Pulse Phenomena* (Academic, San Diego, 1996), Chap. 8.
14. I. P. Christov, J. Zhou, J. Peatross, A. Rundquist, M. M. Murnane, and H. C. Kapteyn, "Nonadiabatic effects in high-harmonic generation with ultrashort pulses," *Phys. Rev. Lett.* **77**, 1743–1746 (1996).
15. I. P. Christov, M. M. Murnane, and H. C. Kapteyn, "Attosecond pulse generation in the single-cycle regime," *Phys. Rev. Lett.* **78**, 1251–1254 (1997).
16. V. T. Platonenko, V. V. Strelkov, G. Ferranti, V. Miceli, and E. Fiordilino, "Control of the spectral width and pulse duration of a single high-order harmonic," *Laser Phys.* **6**, 1164–1167 (1996).
17. E. Fiordilino and V. Miceli, "Laser pulse shape effects in harmonic generation from a two-level atom," *J. Mod. Opt.* **41**, 1415–1426 (1994).
18. W. S. Warren, H. Rabitz, and M. Dahleh, "Coherent control of quantum dynamics: the dream is alive," *Science* **259**, 1581–1589 (1993).
19. B. Kohler, V. V. Yakovlev, Jianwei Che, J. L. Krause, M. Messina, K. R. Wilson, N. Schwentner, R. M. Whitnell, and Yijing Yan, "Quantum control of wave packet evolution with tailored femtosecond pulses," *Phys. Rev. Lett.* **74**, 3360–3363 (1995).
20. C. J. Bardeen, Q. Wang, and C. V. Shank, "Selective excitation of vibrational wave packet motion using chirped pulses," *Phys. Rev. Lett.* **75**, 3410–3413 (1995).
21. K. W. DeLong, R. Trebino, J. Hunter, and W. E. White, "Frequency-resolved optical gating with the use of second-harmonic generation," *J. Opt. Soc. Am. B* **11**, 2206–2215 (1994).
22. J. Fienup, "Improved synthesis and computational methods for computer-generated holograms," Ph.D. dissertation (Stanford University, Palo Alto, Calif., 1975).
23. J. R. Fienup, "Phase retrieval algorithms: a comparison," *Appl. Opt.* **21**, 2758–2769 (1982).
24. W. H. Press, S. A. Teukolsky, W. T. Vetterling, and B. P. Flannery, *Numerical Recipes in Fortran: The Art of Scientific Computing*, 2nd ed. (Cambridge University, New York, 1992), p. 805.
25. R. W. Gerchberg and W. O. Saxton, *Optik* **35**, 237–246 (1972).
26. E. M. Hofstetter, "Construction of time-limited functions with specified autocorrelation functions," *IEEE Trans. Inf. Theory* **IT-10**, 119–126 (1964).
27. Yu. M. Bruck and L. G. Sodin, "On the ambiguity of the image reconstruction problem," *Opt. Commun.* **30**, 304–308 (1979).
28. T. R. Crimmins and J. R. Fienup, "Ambiguity of phase retrieval for functions with disconnected support," *J. Opt. Soc. Am.* **71**, 1026–1028 (1981).
29. T. R. Crimmins and J. R. Fienup, "Uniqueness of phase retrieval for functions with sufficiently disconnected support," *J. Opt. Soc. Am.* **73**, 218–221 (1983).
30. J. R. Fienup, "Reconstruction of an object from the modulus of its fourier transform," *Opt. Lett.* **3**, 27–29 (1978).